Device Linearity Comparison of Uniformly Doped and δ-Doped $In_{0.52}Al_{0.48}As/In_{0.6}Ga_{0.4}As$ Metamorphic HEMTs

Y. C. Lin, Edward Yi Chang, *Senior Member, IEEE*, H. Yamaguchi, Y. Hirayama,
X. Y. Chang, and C. Y. Chang, *Fellow, IEEE*

***Abstract*—The uniformly doped and the δ-doped $In_{0.52}Al_{0.48}As/In_{0.6}Ga_{0.4}As$ metamorphic high-electron mobility transistors (MHEMTs) were fabricated, and the dc characteristics and the third-order intercept point (IP3) of these devices were measured and compared. Due to more uniform electron distribution in the quantum-well region, the uniformly doped MHEMT exhibits a flatter transconductance (G_m) versus drain-to-source current (I_{DS}) curve and much better linearity with higher IP3 and higher IP3-to-P_{dc} ratio as compared to the δ-doped MHEMT, even though the δ-doped device exhibits higher peak transconductance. As a result, the uniformly doped MHEMT is more suitable for communication systems that require high linearity operation.**

***Index Terms*—$In_{0.52}Al_{0.48}As/In_{0.6}Ga_{0.4}As$, linearity, metamorphic high-electron mobility transistor (MHEMT), uniformly doped MHEMT, δ-doped MHEMT.**

I. INTRODUCTION

FOR WIRELESS communication applications, it is important to consider that the devices used in the system may produce nonlinear distortion and thus degrade the signal-to-noise of the system. Consequently, the device structures need to be tailored to improve the RF performance of the system. In recent years, metamorphic high-electron mobility transistors (MHEMTs) have been widely investigated for low-noise and high-power applications [1]–[4]. The main advantage of MHEMT is that it uses a high-indium content $In_xGa_{1-x}As$ channel with In composition ranging from 30% to 80%, which results in higher electron mobility for the device. Therefore, MHEMT offers a low-cost alternative to the high performing but more expensive InP HEMTs.

Delta doping and uniform doping are two typical doping types for HEMTs. The performances of HEMT with these two different types of dopings had been studied before [5], [6]. However, no paper on the linearity performance of these two kinds of HEMTs has ever been reported. The $In_{0.52}Al_{0.48}As/In_{0.6}Ga_{0.4}As$ MHEMTs with different doping profiles are studied in this letter for device linearity comparison. Fig. 1 shows the two kinds of device structures studied: one with uniform doping in the $In_{0.3}Al_{0.7}As$ layer and another one with δ doping between the $In_{0.3}Al_{0.7}As$ and $In_{0.52}Al_{0.48}As$ layers. These wafers were grown by molecular beam epitaxy (MBE) on 3-in GaAs substrates with a InAlAs-graded metamorphic buffer. The $In_{0.52}Ga_{0.48}As$ layer was used as the cap layer with a doping concentration of 3×10^{18} cm^{-3} to get good ohmic contacts. The $In_{0.3}Al_{0.7}As$ Schottky layer has high etch selectivity with the $In_{0.52}Ga_{0.48}As$ cap layer, which provides excellent gate recess uniformity. Dual channels with $In_{0.52}Al_{0.48}As$ spacer layers are designed to increase the current density, provide uniform electron distribution, and improve the device linearity [4], [7].

II. DEVICE FABRICATION

The $In_{0.52}Al_{0.48}As/In_{0.6}Ga_{0.4}As$ MHEMT process can be divided into five major steps:

1) device active region definition;
2) ohmic metal deposition and annealing;
3) wet chemical recess;
4) gate formation by electron beam (EB) lithography;
5) air-bridge formation.

The mesa etch was achieved by using $H_3PO_4/H_2O_2/H_2O$ (5 ml: 1 ml: 40 ml) solution, and ohmic contacts were formed by AuGe/Ni/Au with 30-s 310 °C annealing using hot plates annealing. The gate recess was performed using a highly selective $SA/H_2O_2/H_2O$ (5 g: 1 ml: 90 ml) solution, and the gate length of the devices was 0.3 μm, which was formed by electron beam lithography. The gate metal used was Ti/Pt/Au. Device passivation was performed using plasma-enhanced chemical vapor deposition (PECVD) silicon nitride, and the interconnects were formed using gold-plated air-bridges.

III. RESULTS AND DISCUSSION

The electrical characteristics of the two structures in Fig. 1 were studied and analyzed. Fig. 2 shows the drain-to-source current I_{DS} versus the gate-to-source voltage V_{GS} curves of the 0.3×160 μm^2 $In_{0.52}Al_{0.48}As/In_{0.6}Ga_{0.4}As$ MHEMT devices when biased at $V_{DS} = 1.5$ V. The gate-to-drain breakdown

---

Manuscript received February 14, 2006; revised March 29, 2006. This work was supported by the Ministry of Education, the Ministry of Economic Affairs, and the National Science Council of the Republic of China under Contracts NSC 94-2752-E-009-001-PAE and 94-EC-17-A-05-S1-020. The review of this letter was arranged by Editor J. del Alamo.

Y. C. Lin, E. Y. Chang, and X. Y. Chang are with the Department of Materials Science and Engineering and Microelectronics and Information Systems Research Center, National Chiao Tung University, Hsinchu 30010, Taiwan, R.O.C. (e-mail: edc@mail.nctu.edu.tw).

H. Yamaguchi and Y. Hirayama are with NTT Basic Research Laboratories, Atsugi 243-0198, Japan.

C. Y. Chang is with the Department of Electronics Engineering, National Chiao Tung University, Hsinchu 30010, Taiwan, R.O.C.

Digital Object Identifier 10.1109/LED.2006.877307

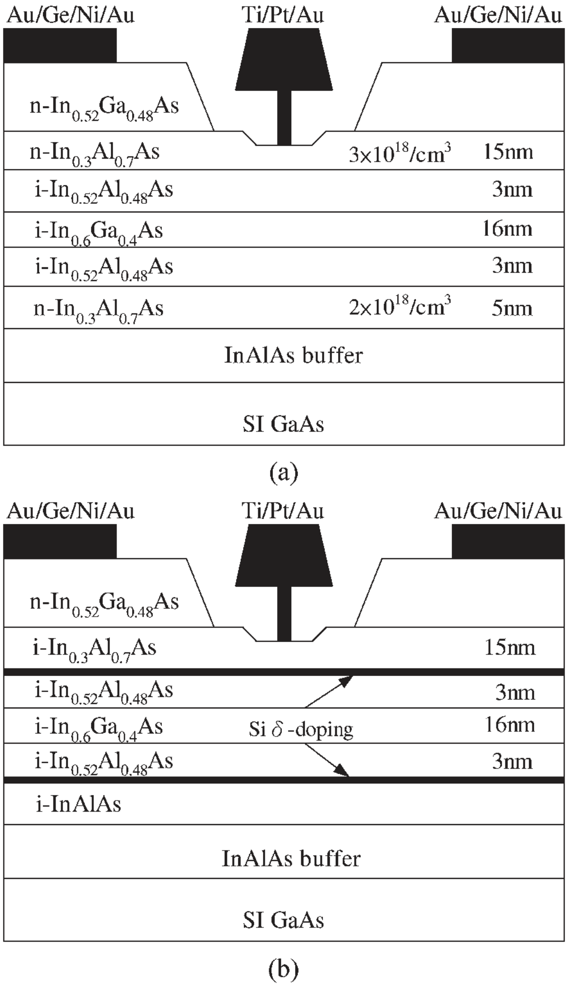

(a)

(b)

Fig. 1. Structure of the $In_{0.52}Al_{0.48}As/In_{0.6}Ga_{0.4}As$ MHEMT. (a) Uniformly doped. (b) δ-doped.

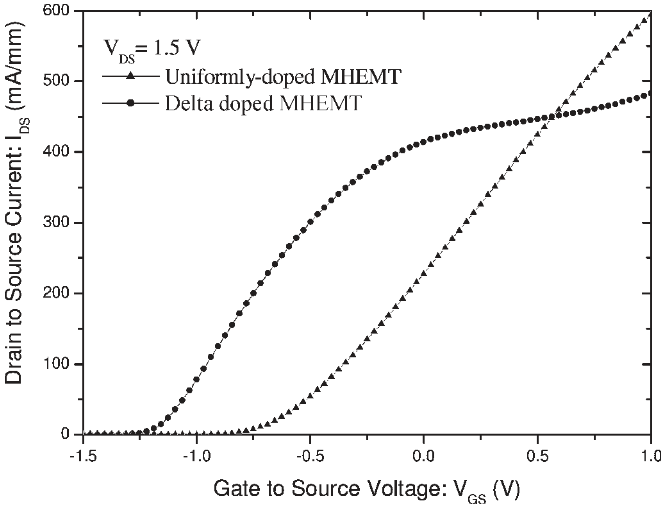

Fig. 2. Drain-to-source current (I_{DS}) versus gate-to-source voltage (V_{GS}) of the 0.3 × 16 μm^2 $In_{0.52}Al_{0.48}As/In_{0.6}Ga_{0.4}As$ MHEMT devices.

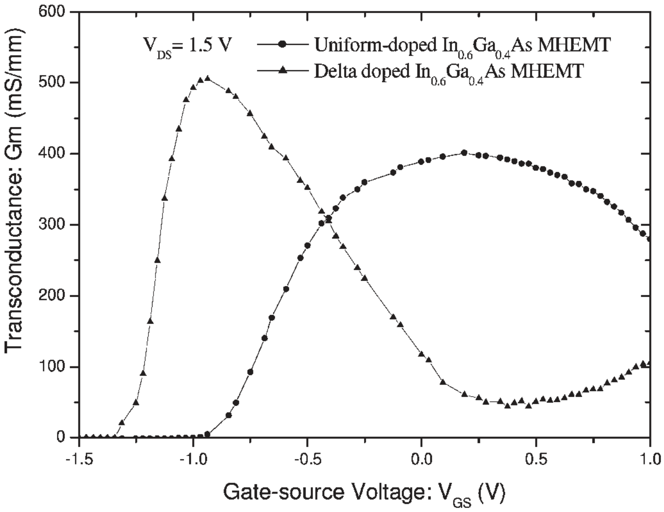

Fig. 3. Extrinsic transconductance (G_m) versus drain-to-source current (I_{DS}) of the 0.3 × 160 μm^2 $In_{0.6}Ga_{0.4}As$ MHEMT devices.

TABLE I
COMPARISONS OF DEVICE PARAMETERS BETWEEN SPC AND MILC TFTs

Parameters*	SPC TFT	MILC TFT
V_{th} (V)	8.2	2.0
S.S. (V/dec)	1.09	0.26
μ_{FE} (cm^2/V.s)	31	201
I_{off}(A)	1.37×10^{-12}	2.26×10^{-12}
I_{on}/I_{off}	7.9×10^{5}	9.7×10^{6}
N_t (cm^{-2})	2.35×10^{12}	5.01×10^{11}

*All parameters were extracted at V_D = 0.5 V except for the off-state current, I_{off}, and ON/OFF ratio, I_{on}/I_{off}, which were extracted at V_D = 3 V. I_{off} is defined as the minimum drain current for convenience.

voltages (BVs) of the δ-doped and the uniformly doped device were 7.2 and 3.8 V, respectively. Compared to the δ-doped device, the uniformly doped device has lower I_{DSS} (I_{DS} at $V_{GS} = 0$) with a more straight I_{DS}–V_{GS} curve. Extrinsic transconductance (G_m) versus gate-to-source voltage (V_{GS}) curves are shown in Fig. 3. Even though the δ-doped device has higher peak G_m, the G_m–I_{DS} curve of the uniformly doped device is flatter than that of the δ-doped device. According to the device simulation results, the uniformly doped device has more uniform electron distribution in the quantum-well region than the δ-doped device. This explains why the uniformly doped device has a flatter G_m–I_{DS} curve. To investigate the linearity performance, the I_{DS}–V_{GS} curves were expressed in terms of a fifth-order polynomial as [8], [9]

$$I_{DS} = a_0 + a_1 V_{GS} + a_2 V_{GS}^2 + a_3 V_{GS}^3 + a_4 V_{GS}^4 + a_5 V_{GS}^5. \tag{1}$$

The device linearity is related to the flatness of the derivative of G_m with V_{GS}, i.e., a_1 should be larger and a_3/a_1 and a_5/a_1 should be minimized. The coefficients of these two devices, which were extracted from the measured data, are listed in Table I. The uniformly doped MHEMT shows higher a_1, lower a_3/a_1, and lower a_5/a_1. Finally, the third-order intercept point (IP3) of these devices were measured to investigate the effect of different types of doping on the device linearity. Because IP3 is a function of several parameters, for comparison, we kept the V_{DS} at 1.5 V, tuning maximum power with different I_{DS} bias for IP3 comparison. Fig. 4 shows the device IP3 with different

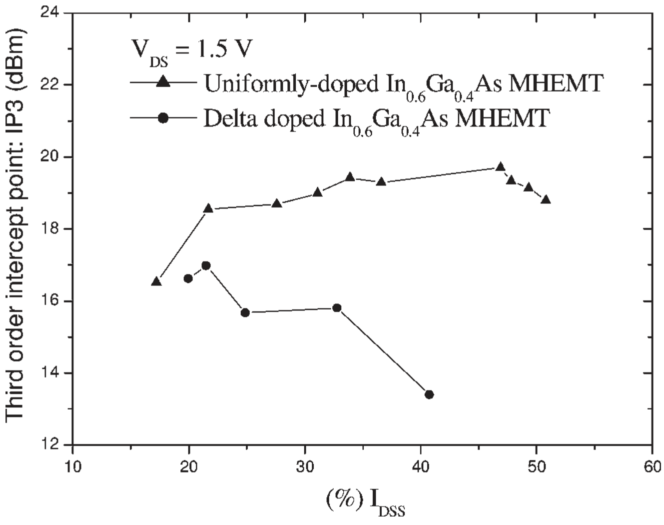

Fig. 4. Comparison of the device linearity of the uniformly doped and the δ-doped $In_{0.52}Al_{0.48}As/In_{0.6}Ga_{0.4}As$ MHEMTs when tested at 6 GHz.

TABLE II
COMPARISON OF THE IP3 OF THE UNIFORMLY DOPED AND THE δ-DOPED $In_{0.52}Al_{0.48}As/In_{0.6}Ga_{0.4}As$ MHEMTS

Device Type	DC bias point: V_{DS} = 1.5V				
	I_{DS} (mA)	Operation frequency: 6GHz			
		P1dB (dBm)	IP3 (dBm)	Δ (IP3-P1dB) (dB)	IP3/PDC
δ doped $In_{0.6}Ga_{0.4}As$ MHEMT	16.72	4.88	16.98	12.1	1.96
Uniformly-doped $In_{0.6}Ga_{0.4}As$ MHEMT	10.32	6.17	19.83	13.66	6.21

bias currents. For IP3 measurement, the load impedance was first tuned for maximum power for each individual device. Then, the third-order intermodulation distortion level (IMD3) was measured and plotted as a function of input power under given dc bias conditions. IP3 was determined by the intercept point of the Pout and IMD3 curves (as functions of input power) after extrapolation. Two signals with the same amplitude but 1 MHz apart in frequency at 6 GHz were used as the input for IMD3 measurement. The uniformly doped MHEMT has higher IP3 as compared to the δ-doped device at a wide range of bias currents. The measured maximum IP3 of the uniformly doped MHEMT was 19.83 dBm, and that of the δ-doped device was 16.98 dBm. A higher Δ (IP3-P1 dB) of 13.66 dB was observed for the uniformly doped MHEMT, compared to the 12.1 dB that was observed for the δ-doped one. In addition, the uniformly doped MHEMT demonstrates a much higher IP3-to-dc power consumption ratio ($IP3/P_{dc}$) of 6.21, as compared to the δ-doped device, which has 1.96 (Table II).

IV. CONCLUSION

The uniformly doped and δ-doped $In_{0.52}Al_{0.48}As/In_{0.6}Ga_{0.4}As$ MHEMTs were fabricated, and the device linearity was compared. Even though the δ-doped device has higher peak transconductance, the uniformly doped MHEMT shows much better device linearity. This is because the uniformly doped device has more uniform electron distribution in the quantum-well region, which enables the device to possess a straight $I_{DS}-V_{GS}$ curve and a flatter G_m-I_{DS} curve, and in turn results in much higher IP3 levels, higher Δ, and higher $IP3/P_{dc}$. Thus, the uniformly doped MHEMT device is more suitable for modern digital wireless communication systems, which impose very stringent linearity requirements for the devices.

REFERENCES

[1] M. S. Heins, J. M. Carroll, M. Kao, J. Delaney, and C. F. Campbell, "X-band GaAs mHEMT LNAs with 0.5 dB noise figure," in *Proc. IEEE MTT-S Dig.*, 2004, pp. 149–152.

[2] C. S. Whelan, W. E. Hoke, R. A. McTaggart, S. M. Lardizabal, P. S. Lyman, P. F. Marsh, T. E. Kazior, "Low noise $In_{0.32}(AlGa)_{0.68}As/In_{0.43}Ga_{0.57}As$ metamorphic HEMT on GaAs substrate with 850 mW/mm output power density," *IEEE Electron Device Lett.*, vol. 21, no. 1, pp. 5–8, Jan. 2000.

[3] C. S. Whelan, P. F. Marsh, W. E. Hoke, R. A. McTaggart, P. S. Lyman, P. J. Lemonias, S. M. Lardizabal, R. E. Leoni, III, S. J. Lichwala, and T. E. Kazior, "Millimeter-wave low-noise and high-power metamorphic HEMT amplifiers and devices on GaAs substrates," *IEEE J. Solid-State Circuits*, vol. 35, no. 9, pp. 1307–1311, Sep. 2000.

[4] E. Y. Chang, Y.-C. Lin, G.-J. Chen, H.-M. Lee, G.-W. Huang, D. Biswas, and C.-Y. Chang, "Composite-channel metamorphic high electron mobility transistor for low-noise and high-linearity applications," *Jpn. J. Appl. Phys.*, vol. 43, no. 7A, pp. L871–L872, Jul. 2004.

[5] S. Karmalkar and G. Ramesh, "A simple yet comprehensive unified physical model of the 2-D electron gas in delta-doped and uniformly doped high electron mobility transistors," *IEEE Trans. Electron Devices*, vol. 47, no. 1, pp. 11–23, Jan. 2000.

[6] K. W. Kim, H. Tian, and M. A. Littlejohn, "Analysis of delta-doped and uniformly doped AlGaAs/GaAs HEMT's by ensemble Monte Carlo simulations," *IEEE Trans. Electron Devices*, vol. 38, no. 8, pp. 1737–1742, Aug. 1991.

[7] F.-T. Chien and Y.-J. Chan, "Improved AlGaAs/InGaAs HFETs due to double doped-channel design," *Electron. Lett.*, vol. 35, no. 5, pp. 427–428, Mar. 4, 1999.

[8] H.-C. Chiu, S.-C. Yang, F.-T. Chien, and Y.-J. Chan, "Improved device linearity of AlGaAs/InGaAs HFETs by a second mesa etching," *IEEE Electron Device Lett.*, vol. 23, no. 1, pp. 1–3, Jan. 2002.

[9] N. B. de Carvalho and J. C. Pedro, "Large- and small-signal IMD behavior of microwave power amplifiers," *IEEE Trans. Microw. Theory Tech.*, vol. 47, no. 12, pp. 2364–2374, Dec. 1999.